

ACTIVE FLOW CONTROL FOR HIGH SPEED JETS USING ADVANCED MODELING COUPLED WITH PIV

Zachary P. Berger

Dept. of Mechanical & Aerospace Engineering
Syracuse University
Syracuse, NY 13244
zpberger@syr.edu

Matthew G. Berry

Dept. of Mechanical & Aerospace Engineering
Syracuse University
Syracuse, NY 13244
mgberry@syr.edu

Patrick R. Shea

Dept. of Mechanical & Aerospace Engineering
Syracuse University
Syracuse, NY 13244
prshea@syr.edu

Mark N. Glauser

Dept. of Mechanical & Aerospace Engineering
Syracuse University
Syracuse, NY 13244
mglouser@syr.edu

Bernd R. Noack

Dept. of Fluids, Thermal & Combustion
Institute PPRIME/CNRS
Poitiers, France
bernd.noack@univ-poitiers.fr

Sivaram Gogineni

Spectral Energies, LLC.
Dayton, OH 45431
sgogineni@spectralenergies.com

ABSTRACT

The current work investigates a Mach 0.6 jet flow field with PIV and simultaneously sampled near and far-field pressure. Two component velocity measurements are taken in the streamwise (r - z) plane of the jet. Three cameras are placed such that each interrogation window is captured simultaneously and stitched together to capture a six diameter (D) PIV window. In addition, active flow control is applied using an actuation glove comprised of synthetic jet actuators. Both open and closed-loop control are applied in different physical forcing configurations. For closed-loop control, hydrodynamic pressure from the near-field array of sensors is fed back to the actuation system in real time. The large window PIV allows one to examine how the flow field is affected by the flow control. Low-dimensional modeling techniques, in the form of proper orthogonal decomposition, are performed in order to obtain a better understanding of the large scale, energetic events in the flow field. It has been found that active flow control changes the potential core length and shear layer expansion, which affects the overall sound pressure levels in the far-field.

INTRODUCTION

In recent years, the aerospace community has invested an increasingly large amount of time and resources into research focusing on the jet noise problem. For commercial applications, environmental pollution and increasing amounts of air traffic make jet noise reduction a high priority. From the military perspective, tactical maneuvers and the hearing loss experienced by aircraft carrier flight deck crews motivate an increased interest in the jet noise prob-

lem. Moreover, due to increasingly stringent noise regulations on aircraft in both the private and commercial sectors, jet noise research is more important than ever. The International Civil Aviation Organization is not only calling for quieter aircrafts, but according to Viswanathan & Pilon (2011), the studies should focus on gaining insight into noise source mechanisms and low-noise designs. The turbulence community continues to be at the forefront of these studies, focusing on noise source identification and far-field acoustic noise suppression.

Previous studies have shown that the key to reducing jet noise lies in understanding the physics of the structures created in the region of the collapse of the potential core (Tinney et al. (2008a,b); Tam et al. (2008); Low et al. (2011)). A deep understanding of how these noise producing events propagate to the far-field is paramount. Up to this point, the community has seen various passive control methods for jet noise suppression, typically in the form of chevrons (Brown et al. (2006); Callender et al. (2005); Mengle (2005)). In recent years, the focus has shifted to active flow control. While open-loop control has its benefits, many researchers in the community believe that closed-loop control will provide the most promising results, drawing on intelligence from the system (Samimy et al. (2010); Laurendeau et al. (2008); Low et al. (2010)). At Syracuse University, an actuation glove consisting of eight synthetic jet actuators (based on the designs of Glezer & Amitay (2002) and Smith & Glezer (1998)), is placed on the jet nozzle in order to provide a shear layer excitation.

The motivation for this work stems from a large time-resolved PIV data set collected in 2011 (Low et al. (2013)). During this set of experiments, 10 kHz time-resolved PIV

August 28 - 30, 2013 Poitiers, France

measurements were collected simultaneously with near and far-field pressure. Using POD, “loud” modes in the flow were identified by correlating the time-dependent POD coefficients with the far-field acoustics. Windowing effects from the TRPIV experiments led to curiosity of a larger view of the flow-field and thus a large window PIV data set was collected.

EXPERIMENTAL SETUP

Experiments were conducted in the Syracuse University anechoic chamber at the Skytop campus. The anechoic chamber housing the jet facility is 206 m³ and is lined with fiberglass wedges having a cutoff frequency of 150 Hz. The chamber houses an axisymmetric matched 5th order polynomial nozzle with a diameter of 2 inches (50.8 mm) as described by Tinney et al. (2004). The anechoic chamber can be seen in Figure 1.



Figure 1. Syracuse University Anechoic Chamber

For hydrodynamic pressure measurements in the near-field, two azimuthal arrays of Kulite pressure transducers are used, each consisting of five sensors located at $x/D = 6$ and 8. All sensors are placed 1cm outside of the expanding shear layer to measure the hydrodynamic pressure. The azimuthal array of sensors at $x/D = 6$ are used for feedback in the closed-loop control. For far-field acoustic sensing, twelve G.R.A.S. microphones are used in two arrays. The first six microphones are in the plane of the jet and the second array is offset by 15° out of plane with respect to the jet. For each array, the microphones are spaced evenly from 15° to 90° with respect to the jet axis. All microphones are located 75D downstream of the nozzle lip. This configuration can be seen in Figure 1.

Velocity measurements are acquired using a standard 4 Hz Dantec Dynamics Particle Image Velocimetry (PIV) system with three cameras for an extended interrogation window. Two component velocity measurements are collected in the streamwise plane of the jet to obtain a six diameter window. The three individual windows are stitched together during post-processing, using a least-squares approach, to obtain the large window.

For active flow control, an actuation glove comprised of a circular array of eight synthetic jet actuators has been designed and optimized. These zero net mass flux actuators have the ability to achieve exit velocities on the order of 50-60 m/s, which are sufficient to disturb the developing shear layer. The synthetic jets have been designed such that each actuator can be controlled independently for high modal forcing. The actuation glove can be seen in Figure 2, and further information regarding the actuation system is outlined in Low et al. (2013).

In the current investigation, each azimuthal pressure array contains five sensors and therefore modes 0 and 1 are



Figure 2. Actuation Glove for Flow Control

implemented to avoid spatial aliasing. Four different control schemes, two open-loop and two-closed loop, are implemented to see the effects of the control on the flow-field with a large window, as well as to see how control effects the far-field noise. There are two different types of physical forcing implemented for both open and closed-loop control. The first is a mode 0 forcing in which all actuators are driven in phase to mimic a column mode forcing. The second is a mode 1 forcing in which half of the actuators are driven 180° out of phase to mimic a flapping mode. The driving signal for the actuators is a sine wave driven at 1200 Hz (preferred frequency of the synthetic jet actuators). For closed-loop control, the original driving signal is amplitude modulated using the real time Fourier-filtered modes of the near-field azimuthal pressure at $x/D = 6$.

RESULTS

Two control cases will be focused on in the following section, one open-loop and one closed-loop, to be compared with the uncontrolled jet. For the open-loop case, a mode 1 physical forcing is applied. In this particular scenario, the top four actuators are driven 180° out of phase from the bottom four actuators to create a flapping mode forcing about the x-axis. For the closed-loop case, the Fourier-filtered mode 0 of the near-field pressure array at $x/D = 6$ is fed back to the actuators, which are driven again with a mode 1 forcing.

Low-dimensional models are incredibly important in the fluid mechanics community especially when one is interested in extracting large scale, dominant flow structures of a complex flow field. When looking at the jet noise problem specifically, reduced-order modeling is essential due to increasingly large data sets and complex flow physics. In order to develop a low-dimensional model of the flow field, proper orthogonal decomposition (POD) is implemented. POD was first introduced into the turbulence community by Lumley (1967) and later simplified by Sirovich (1987) using the concept of snapshots. The snapshot approach is useful when the number of grid points is greater than the number of snapshots. In this modified approach the problem becomes a temporal formulation instead of spatial, and thus becomes more computationally manageable. The mathematical formulation of the snapshot POD is described in detail by Low et al. (2013).

Large Window PIV

For the PIV acquisition, three cameras were placed side by side to acquire three independent windows, each spanning approximately two diameters in the streamwise direction. In order to create one large window from these

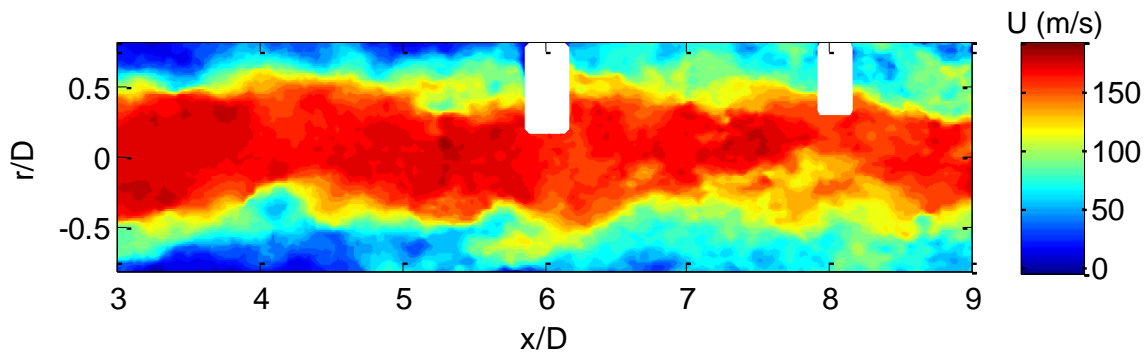


Figure 3. Large Window PIV Baseline Snapshot

three separate images, the windows needed to be stitched together; this process is done in three main steps. First an appropriate offset between the windows is determined, then an appropriate scaling factor for the velocities in the overlap region is calculated, and finally the images are stitched together. The stitching is performed by interpolating the images onto a large grid using a weighted average scheme. An example of the resulting large window PIV image for the baseline case can be seen in Figure 3. The blanked regions at six and eight diameters in the window are from the azimuthal array of Kulites. These sensors are out of the PIV plane but show up in the images and are therefore blanked out for purposes of the POD analysis.

In order to see the effects of the control on the flow-field, the mean flow for the different cases is observed in Figure 4. The plots show the mean streamwise velocity contours for the baseline and two control cases. In the uncontrolled jet, the potential core collapses just before 8D, whereas for the open-loop and closed-loop cases, the potential core is shortened to about 6D and 6.5D, respectively. This shows that with the current control schemes, the potential core length has been significantly reduced. Though the two control cases seen here seem to have a similar effect on the flow field, a control strategy which requires less energy input to the system is desired.

By looking at the RMS of the actuation input signals, the closed-loop control requires less energy input to the system, having an RMS value of 2.75 volts as compared to 3.08 volts for the open-loop. Moreover, the closed-loop control draws on intelligence from the system and therefore makes this more desirable than open-loop from an active control standpoint. In the open-loop case, one might notice a slight vectoring of the jet in the upwards direction. The reason for this vectoring is still being investigated however one explanation is that the driving of the actuators induces an initial condition which causes a slight vectoring of the jet in the open-loop case. It is possible that this wouldn't be seen in the closed-loop case since the feedback allows for the control system to turn on and off. Once again, these concepts are being investigated but at this point the actuation input is thought to be the cause of vectoring in the open-loop case.

Near-Field Pressure Spectra

The collapse of the potential core at approximately six and eight diameters for the control and baseline, respectively, motivates the investigation of the near-field pressure at these locations. For comparisons, the near-field pres-

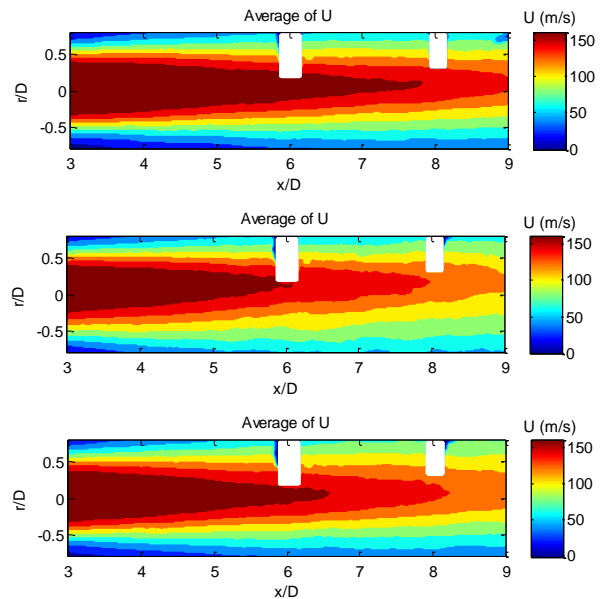


Figure 4. Streamwise Velocity Contours of Mean Flow: Baseline (top), Open-Loop (center), Closed-Loop (bottom)

sure spectra at $x/D = 8$ for the baseline and $x/D = 6$ for the closed-loop control are shown in Figure 5. The arrangement of the Kulites with respect to the jet can be seen in Figure 6, corresponding to the colors in Figure 5. Similar trends are observed for the two cases and the sensors all collapse quite well indicating symmetry throughout the array. For the baseline case, the array is just beyond the collapse and therefore there is a slight amplitude shift in some of the sensors. For the closed-loop case, the dominant frequency is preserved however there is a noticeable increase in overall energy. This is not only attributed to the fact that these sensors are closer to the jet exit, but also the control has increased the spreading rate of the jet, accounting for the additional energy increase seen by the sensors. Despite the fact that a mode 1 physical forcing is applied, the feedback of Fourier mode 0 keeps the flow relatively axisymmetric across the entire frequency band.

POD Analysis

Performing the POD analysis on this data set provides information about the low-dimensional, highly energetic structures in a large region of the flow field where the flow physics change dramatically. From the POD, it is found that

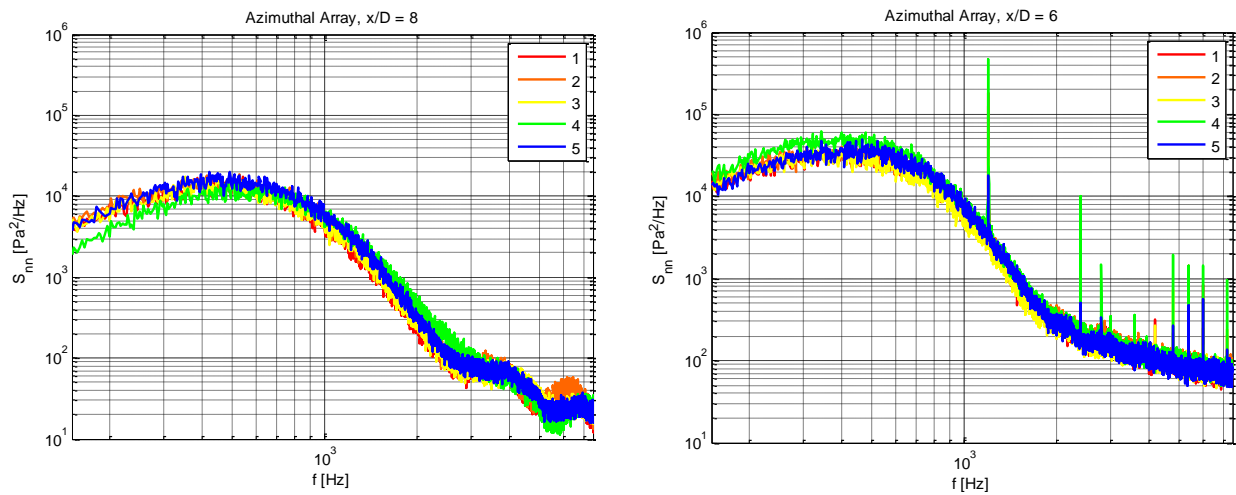


Figure 5. Near-Field Pressure Spectra: Baseline, $x/D = 8$ (Left), Closed-Loop, $x/D = 6$ (Right)

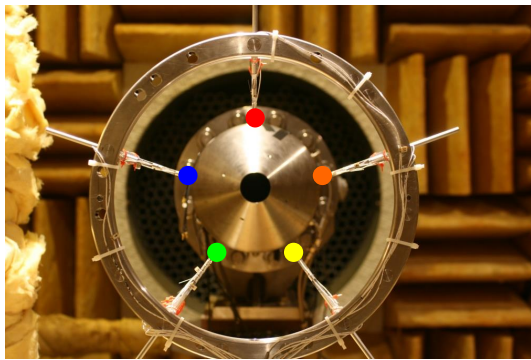


Figure 6. Near-Field Pressure Sensors

there is a favorable convergence rate of the eigenvalues, as about 50% of the total energy is recovered with just over 20 modes (of the total 300). In addition, the analysis shows that none of the individual modes contain more than 6% of the total energy.

The first two spatial eigenfunctions (POD modes) for the baseline and closed-loop control cases are shown in Figure 7. These two modes are the highest in energy and are the fundamental building blocks of the flow field. For the baseline flow, the development of large scale vortices can be seen along the shear layer beginning near the collapse of the potential core. In the closed-loop configuration, small scale vortices can be seen along the shear layer across the entire PIV window. In addition, the mode 1 forcing can be observed by the opposite phase of the structures seen in the top and bottom shear layers. Beyond the collapse of the potential core the structures grow and become less organized due to the interaction of the vortices caused by the collapse. Interestingly enough, the mode 1 forcing with feedback from Fourier mode 0, keeps the flow organized and greatly enhances the overall mixing in the shear layer.

Using a select number of POD modes, the velocity field can be reconstructed as shown in Figure 8. The baseline is shown on the left and the closed-loop on the right. The top plot shows the fluctuating velocity contours in the streamwise direction. The bottom plot shows the 25 mode reconstruction, which accounts for just over 50% of the total en-

ergy. As can be seen in both the baseline and closed-loop cases, the large scale structures are represented accurately with the reconstruction. From these plots, it can be seen that the closed-loop control keeps the flow organized before the collapse, as observed in the reconstructions. The mode 1 forcing causes the potential core to collapse sooner, evident in even a single snapshot. The advantage to the large window PIV is that it allows one to examine the flow structures before and after the collapse of the potential core without windowing effects (which can be problematic in standard sized PIV windows).

Far-Field Sound Pressure Levels

In order to quantify differences in sound pressure level for the various control cases, a directivity plot of the far-field microphones is presented. This plot shows the change in overall sound pressure level at each of the far-field microphones with respect to the baseline (uncontrolled) jet. Presented here is the directivity plot for the in-plane microphones, with similar trends observed for the out-of-plane microphones. As can be seen in Figure 9, despite the fact that none of the control cases provide a reduction in far-field noise, control authority over the jet is evident. Moreover, the different control cases seem to exhibit a directivity effect which is to be expected, as different forcing and feedback mechanisms are provided for the control input. The various types of forcing applied tend to enhance mixing and therefore change the structures being propagated to the far-field due to a shift in the potential core length and growth of the shear layer.

Focusing on the microphone at 15 degrees where the sound pressure level is largest, it can be seen that the closed-loop control case in which Fourier mode 0 is fed back to physically force mode 1, is the closest to the baseline. In addition, an open-loop forcing of mode 1 seems to be the loudest control case at this particular microphone. As was observed from the mean velocity field and POD analysis, with active flow control (both open and closed-loop), the potential core length has been significantly shortened and a slight increase in the shear layer expansion is also observed. Subtle changes between the open and closed-loop control can be accounted for by the feedback mechanism present in the closed-loop case. These subtle changes clearly result in

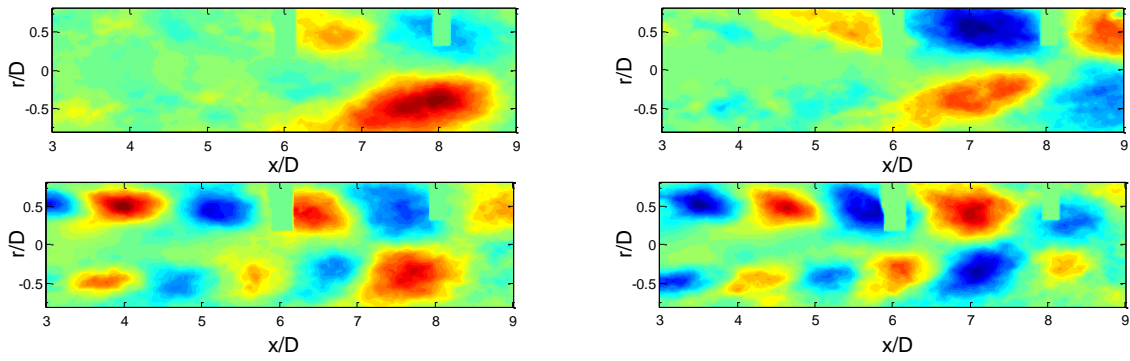


Figure 7. Spatial POD Modes: Mode 1 (left column), Mode 2 (right column); Baseline (top), Closed-Loop (bottom)

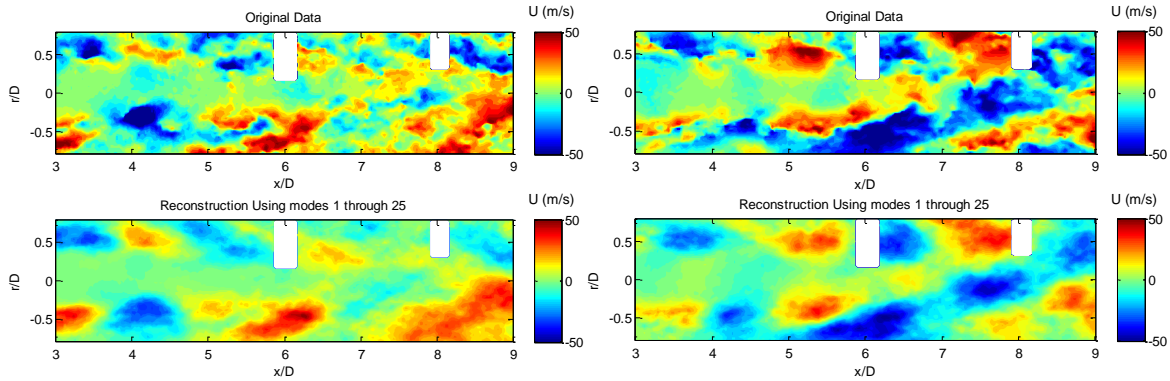


Figure 8. Fluctuating Velocity Reconstructions: Baseline (Left), Closed-Loop (Right)

slight differences in the overall sound pressure levels in the far-field and requires further investigation.

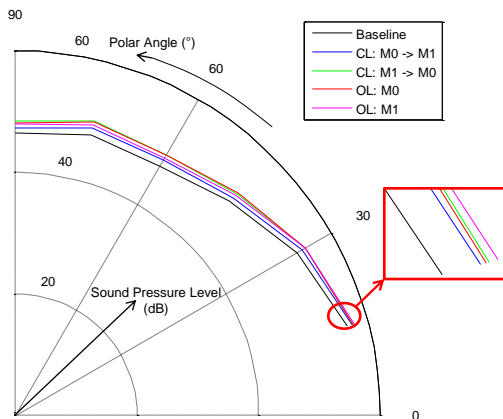


Figure 9. Sound Pressure Level Directivity: In-plane Microphones

DISCUSSION

Previous investigations into the jet flow field using standard PIV techniques have shown limiting analysis capabilities due to the small window sizes. Here, a large PIV window comprised of six jet diameters has been presented and analyzed to help gain insight into the flow structures being created as a result of the collapse of the potential core.

In addition, simultaneous near and far-field pressure measurements were acquired with both open and closed-loop flow control. Mean velocity contour profiles indicate that the potential core of the jet has been significantly shortened using active flow control. Moreover, since the closed-loop control uses less input energy and draws on intelligence from the flow field, this becomes a more desirable control option than open-loop, for jet noise applications. This is further validated by the fact that the closed-loop control case has a lower overall sound pressure level in the far-field across all of the in-plane microphones, as compared to the open-loop case. The POD analysis shows that a large amount of the total energy of the system can be recovered with a small amount of modes. Looking at the first two POD modes indicates that the closed-loop control keeps the flow organized until the collapse of the potential core.

Additional Large Window Analyses

In order to take the results presented a step further, an LSE-based approach will be implemented in order to build a time-resolved view of the flow field based on the near-field pressure. This will provide additional insight into the flow field and allow for comparisons to be made to the time-resolved experiments of 2011. The advantage is that a time-resolved, large window field will be developed to explore which modes may be the “loud” modes in the flow field. In addition, these results can be compared to those of the previous experiments for validation and further investigation.

With all of the toolkits described thus far for analyzing the flow field, a more mathematically rigorous method for defining low-dimensional flow structures that account for the far-field noise is desirable. For this analysis, a reduced order modeling technique known as OID (observable

inferred decomposition) will be applied to this data set. The details of the OID can be found in the works of Jordan et al. (2007) and Schlegel et al. (2012). Moreover, vorticity in the large window will also be explored to better understand how the interaction of structures created by the potential core collapse, contribute to noise producing events.

Further Exploration of the Flow Field

To complement the time-resolved experiments of 2011 (Low et al. (2013)), as well as the experiments presented here, an additional time-resolved PIV data set has been acquired at Syracuse University. The motivation for this data set is two-fold. The first part of the analysis will focus on combining large window PIV with time-resolved PIV, alongside open and closed-loop control. This will help to further analyze the effect of control on the flow structures in the collapse region. The second aspect to be explored is a three-dimensional reconstruction of the jet flow field, using large window time-resolved measurements in the radial direction, and simultaneous near-field pressure. With a global view of the flow field, much insight can be gained into the mechanisms responsible for the noise, which are generated in the region of the collapse of the potential core. This analysis, along with the observations from the control presented here, should provide the necessary tools for designing a more effective controller for far-field jet noise reduction. Since control authority over the flow field has been demonstrated and “loud” modes in the flow have been identified, the key is to now gain a deeper understanding of the flow physics related to the noise producing events in the flow.

ACKNOWLEDGEMENTS

The authors would like to acknowledge Spectral Energies, LLC. Phase II SBIR, with AFRL, Dr. Barry V. Kiel as project monitor, for the ongoing support and interactions throughout these research endeavors. The authors also acknowledge Dr. Jacques Lewalle and Christopher Ruscher (Syracuse University) for many insightful discussions throughout the experiments and analysis. Lastly, the authors acknowledge the ANR Chair of Excellence TUCOROM for funding and excellent working conditions.

REFERENCES

Brown, C.A., Bridges, J., *Acoustic efficiency of azimuthal modes in jet noise using chevron nozzles*. 12th AIAA/CEAS Aeroacoustics Conference (27th AIAA Aeroacoustics Conference), (2645), 2006.

Callender, B., Gutmark, E., Martens, S., *Far-field acoustic investigation into chevron nozzle mechanisms and trends*. AIAA Journal, 43(01), 87-95, 2005.

Glezer, A., Amitay, M., *Synthetic Jets*. Annual Review of Fluid Mechanics. 34: 503-529 (2002).

Jordan, P., Schlegel, M., Stanlov, O., Noack, B.R., Tinney, C.E., *Identifying noisy and quiet modes in a jet*. 13th

AIAA/CEAS Aeroacoustics Conference (28th AIAA Aeroacoustics Conference), (3602), 2007.

Laurendeau, E., Jordan, P., Bonnet, J.P., Delville, J., Parnaud, P., Lambalais, E., *Subsonic jet noise reduction by fluidic control: The interaction region and the global effect*. Physics of Fluids, 20(101519):1-15, 2008.

Low, K.R., El-Hadidi, B., Glauser, M.N., Andino, M.Y., Berdanier, R., *Investigation of different active flow control strategies for high speed jets using synthetic jet actuators*. 40th Fluid Dynamics Conference and Exhibit, (4267), 2010.

Low, K.R., Berger, Z.P., Lewalle, J., El-Hadidi, B., Glauser, M.N., *Correlations and Wavelet Based Analysis of Near-Field and Far-Field Pressure of a Controlled High-Speed Jet*, AIAA 2011-4020, 41st AIAA Fluid Dynamics Conference and Exhibit, Honolulu, HI, June 27-30, 2011.

Low, K.R., Berger, Z.P., Kostka, S., El Hadidi, B., Gogineni, S., and Glauser, M., “A low-dimensional approach to closed-loop control of a Mach 0.6 jet,” *Experiments in Fluids*, Vol. 54, pp. 1-17, 2013.

Lumley, J.L., “The structure of inhomogeneous turbulent flows,” *Atm. Turb. and Radio Wave Prop.*, Yaglom AM, Tatarsky VI (eds) Nauka, Moscow, pp. 166-178, 1967.

Mengle, V.G., *Jet noise characteristics of chevron in internally mixed nozzles*. 11th AIAA/CEAS Aeroacoustics Conference (2934), 2005.

Samimy, M., Kim, J.H., Fischer, M.K., Sinha, A., *Acoustic and flow fields of an excited high reynolds number axisymmetric supersonic jet*. Journal of Fluid Mechanics, 656:507-529, 2010.

Schlegel, M., Noack, B.R., Jordan, P., Dillmann, A., Groschel, E., Schroder, W., Wei, M., Freund, J.B., Lehmann, O., Tadmor, G., *On least-order flow representations for aerodynamics and aeroacoustics*. Journal of Fluid Mechanics: Vol 679, pp. 367-398, 2012.

Sirovich, L., *Turbulence and the Dynamics of Coherent Structures: I, II and III*, Quarterly Applied Mathematics, 45, pp.561, 1987.

Smith, B.L., Glezer, A., *The formation and evolution of synthetic jets*. Physics of Fluids. 10(9): 2281-97 (1998).

Tam, C.K.W., Viswanathan, K., Ahuja, K.K., Panda, J., *The sources of jet noise: experimental evidence*. Journal of Fluid Mechanics. vol. 615, pp. 253-292.

Tinney, C.E., Hall, A., Glauser, M.N., Ukeiley, L.S., Coughlin, T., *Designing an anechoic chamber for the experimental study of high speed heated jets*, 42nd AIAA Aerospace Sciences Meeting and Exhibit, AIAA 2004-0010, 2004.

Tinney, C.E., Glauser, M.N., Ukeiley, L.S., *Low-dimensional characteristics of a transonic jet: Part 1. Proper Orthogonal Decomposition*. Journal of Fluid Mechanics, 612, 107-141. 2008.

Tinney, C.E., Ukeiley, L.S., Glauser, M.N., *Low-dimensional characteristics of a transonic jet: Part 2. Estimate and far-field prediction*. Journal of Fluid Mechanics, 615, 53-92. 2008.

Viswanathan, K. and A. Pilon., *Aeroacoustics*, Aerospace America: Year in Review 2011. Dec. 2011.